Available online at www.sciencedirect.com
SCIENCE DIRECT®

Journal of the European Ceramic Society 26 (2006) 981–986

www.elsevier.com/locate/jeurceramsoc

Electrochemical decomposition of NO over composite electrodes on YSZ electrolyte

Hwa-Seob Song[a], Jooho Moon[a,*], Hae Jin Hwang[b]

[a] *School of Advanced Materials Science and Engineering, Yonsei University, Seoul 120-749, Republic of Korea*
[b] *Department of Ceramic Engineering, Inha University, Incheon 402-751, Republic of Korea*

Received 7 June 2004; received in revised form 22 November 2004; accepted 5 December 2004
Available online 23 February 2005

Abstract

NO decomposition over electrochemical cells that involve a bilayered composite electrode has been investigated. NO was decomposed only after a minimum current density was applied and its conversion increased abruptly with increasing applied current. The compositions of phases and their spatial distribution on the cathode strongly influenced the decomposition activity as a function of the current density since they are directly correlated with the site and number densities of the triple-phase boundary and the electrochemically induced active site, i.e., F-center. The [($La_2Sn_2O_7$ + YSZ)/Pt] electrode could convert more than 85% of NO into N_2 at 200 mA/cm^2 whereas only 27% was decomposed over the platinum electrode although the latter was more electrochemically active at lower current ~70 mA/cm^2. The addition of Pt into the [($La_2Sn_2O_7$ + YSZ)/Pt] composite electrode not only expands the densities of the *tpb* and F-centers but also enhances competitive NO adsorption as indirectly confirmed by impedance spectroscopy, both of which promote NO conversion at the lower current density.

Keywords: ZrO_2; Electrode; Membrane; $La_2Sn_2O_7$; NO

1. Introduction

Significant research has been focused on solid-state electrochemical cells as an alternative approach to the reduction of harmful NO gases from combustion emission.[1] The electrocatalytic reduction of NO over a Pt electrode deposited on a stabilized zirconia solid electrolyte was first proposed by Huggins and co-workers.[2] By applying a direct electric potential, NO is directly reduced at the cathode forming gaseous N_2 and the oxygen produced was ionized and pumped through the solid electrolyte to the anode. This indicates that NO can be simply decomposed without the aid of a reducing agent and its reaction rate can be controlled electrically. In the presence of excess oxygen, however, higher current density is required for NO reduction, decreasing its current efficiency because the coexisting oxygen is preferentially adsorbed and decomposed at the cathode.

The electrochemical reduction of NO is supposed to involve dissociate adsorption at the triple-phase boundary (*tpb*) on the cathode surface and desorption of N_2 to the gas phase.[3,4] The remaining adsorbed oxygen atom diffuses to a neighboring oxygen vacancy, at which the oxygen atom is incorporated as an oxygen ion into the lattice by combining with trapped electrons at the vacancy site. This electrochemical active site is an F-center (V_O^x). The overall reaction can be represented as $NO + V_O^x \rightarrow O_O^x + \frac{1}{2}N_2$. The oxide ion is then transported through the solid electrolyte to the anode where O_2 is formed and ejected. It is believed that the dissociate adsorption of NO and the N_2 desorption occur quite rapidly, whereas the diffusion and the ionization of the adsorbed oxygen are relatively sluggish.[5] Therefore, in order to selectively reduce NO with high current efficiency, the cathode surface should have an affinity towards NO adsorption even in the

---

[*] Corresponding author. Tel.: +82 2 2123 2855; fax: +81 2 365 5882.
E-mail address: jmoon@yonsei.ac.kr (J. Moon).

0955-2219/$ – see front matter © 2005 Elsevier Ltd. All rights reserved.
doi:10.1016/j.jeurceramsoc.2004.12.026

coexistence of O_2. The surface concentration of the oxygen vacancies located nearby the *tpb* and their mobility also play critical roles in determining the catalytic activity for NO decomposition. Furthermore it is necessary to expand the effective lengths of the *tpb* by generating three-dimensional pathways for both ionic and electronic conductions, so that the electrochemical reduction reaction can occur across the entire cathode surface.[6]

In this respect, many attempts to enhance the electrocatalytic efficiency are being pursued by utilizing either metal-oxide composites such as Pt-Ga_2O_3, oxide-oxide composites such as NiO-YSZ, or mixed ionic electronic conductors (MIEC) such as $LaCoO_3$, $La_{0.6}Sr_{0.4}Co_{0.2}Fe_{0.8}O_3$ (LSCF), and $La_{0.8}Sr_{0.2}Co_{0.9}Ru_{0.1}O_{3-\delta}$.[4,7–12] In the present study, we have designed a electrochemical cell in which the cathode is composed of a mixture of Pt, YSZ, and lanthanum stannate pyrochlore ($La_2Sn_2O_7$, LSO). The Pt acts as an electronic conductor as well as a competitive adsorption site for NO in the presence of O_2 whereas the YSZ plays a role as an ionic conductor, the combination of these phases endowing a mixed conductivity to the cathode, increasing the site density of the *tpb*. The LSO is used as a catalyst for the direct decomposition of NO at high temperatures (>400 °C).[13] It possibly provides active sites for NO adsorption and decomposition since it has intrinsic oxygen vacancies (8 per unit cell) present in the pyrochlore lattice.[14] Using such an electrochemical cell we tried to distinguish the roles of each component contributing to the electrochemical reduction of NO.

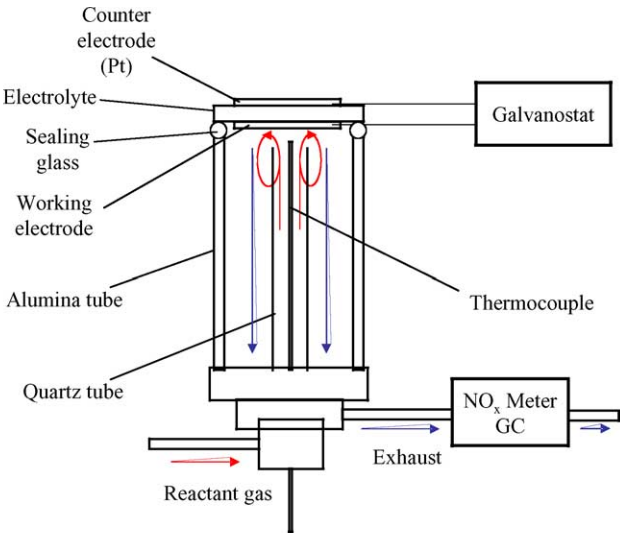

Fig. 1. Configuration of an electrochemical cell and characterization system for NO decomposition.

2. Experimental

A commercially available yttria stabilized zirconia (YSZ) disk (Tosoh TZ8Y, diameter = 20 mm, thickness = 0.5 mm) was used as the oxygen conducting solid electrolyte. The electrochemical cells involving different compositions were produced by applying a paste material onto the YSZ disk. Two kinds of electrocatalytic electrodes were investigated, namely, a binary mixed composite of hydrothermally-derived LSO[15] which was well-crystallized phase-pure pyrochlore oxide with the mean particle size of 0.59 μm and YSZ (Tosoh, TZ8Y) in a volume ratio of 3:2 and a ternary mixed composite of LSO, YSZ, and Pt (Aldrich Chemicals) in a volume ratio of 2:2:1. The pastes were prepared by dispersing these powders in α-terpineol together with ethyl cellulose as a binder followed by milling using a three roller mill (EXAKT 35).

The cathodes were fabricated in a bilayered structure. The platinum paste was screen-printed as a circle with 14 mm diameter on the YSZ disk and fired at 1000 °C for 1 h to form a current distributing layer.[16] The thickness of the platinum electrode was approximately 3.5 μm. The electrocatalytic composite layer of two different compositions was then screen-printed over the underlying Pt layer and sintered at 1400 °C for 4 h, resulting in ~8 μm-thick bilayered cathode. A cell with ~10 μm-thick single-layered Pt cathode was also prepared to compare the electrocatalytic behavior with those of the bilayered composite electrodes. The anode was the Pt applied on the other side of the YSZ disk fired at 1000 °C for 1 h, and the platinum wire for current lead line was contacted with the platinum layers at both sides. Three electrochemical cells studied in the present study are denoted as (LSO + YSZ)/Pt (cathode)|YSZ|Pt (anode), (LSO + YSZ + Pt)/Pt|YSZ|Pt, and Pt|YSZ|Pt.

The electrochemical cell was mounted on an alumina tube reactor followed by sealing with glass in a furnace at 1000 °C as shown in Fig. 1. The reactant gases of 0.1% NO and 2% O_2 balanced with He were introduced at 700 °C while applying a constant direct current to the cell by galvanostat. The flow rate was 50 ml/min and the flow rate of each reactant gas was controlled by mass flow controllers (Bronkhorst, F-201C). Experiments were carried out at reaction temperatures from 550 to 700 °C, monitored by a K-type thermocouple inserted into the alumina tube. The reactor was equilibrated for 20 min before any measurement at each applied current. The NO and O_2 concentrations in the exhaust gas were monitored by on-line gas chromatography (GC, Varian CP-2002) and NO_x analyzer (Horiba CLS-510) to determine the NO decomposition by electrochemical reaction. AC impedance spectroscopy (Solatron SI 1260/ SI 1287) was used to measure the resistance of the electrochemical cell associated with the NO decomposition characteristics. Impedance spectra were taken in the frequency range of 0.01 Hz to 100 kHz, and the applied ac amplitude was set to 20 mV while supplying the constant current to the cell in the same reaction atmosphere. The Pt reference electrode applied on the opposite side of the electrocatalytic electrode was used during the impedance measurement. Microstructure and compositional distribution in the electrochemical cells before and after the reaction were observed by scanning electron microscopy (SEM, S-4200, Hitachi) and electron probe microscopic analyzer (EPMA, JXA-8600, JEOL), respectively.

3. Results and discussion

Fig. 2 shows the microstructure of the electrochemical cells of three different electrode compositions before and after sintering. Submicron-sized Pt particles underwent significant densification, forming a metal electrode with larger grain structure as shown in Fig. 2(a) and (b). Initially larger LSO and smaller YSZ particles were relatively well-mixed in the as-screen printed electrode (Fig. 2(c)). Upon sintering particle necks between LSO and YSZ grew to produce a porous composite electrode with three-dimensionally interconnected network structure (Fig. 2(d)). Adding fine Pt particles into the (LSO + YSZ) composite electrode seems to decrease the porosity to some extent by filling the interstices between the larger particles as seen in Fig. 2(e) and (f). The thickness of these three electrodes was in the range of 8–10 μm when sintered at 1400 °C for 4 h.

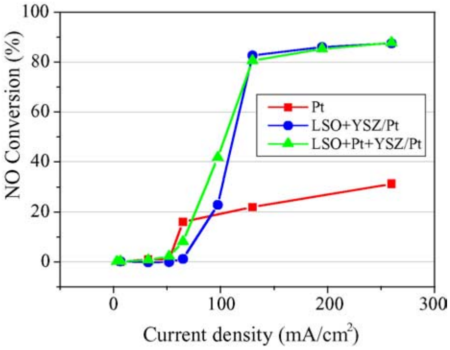

Fig. 3. NO decomposition as a function of the applied current for different electrodes in the electrochemical cells.

Fig. 3 shows NO decomposition behavior as a function of the applied current for the electrochemical cells. There was a threshold current required to initiate NO decomposition for all the cells. NO removal by electrochemical reaction did not occur when insufficient current was applied, whereas the decomposition started at 50–60 mA/cm^2. NO conversion over Pt|YSZ|Pt was as high as 32% at 300 mA/cm^2 and the decomposition started at lower current density than for the other electrode materials. For the two electrochemical cells involving the composite electrodes, NO decomposition behavior as a function of the applied current was observed to be similar. In the case of (LSO + YSZ + Pt)/Pt|YSZ|Pt, however, NO decomposition started at 60 mA/cm^2 and its conversion increased abruptly when a higher current density above 60 mA/cm^2 was supplied to the cell, reaching to ∼87% conversion at 250 mA/cm^2.

The existence of a threshold current density to initiate decomposition indicates that the oxygen is preferably adsorbed

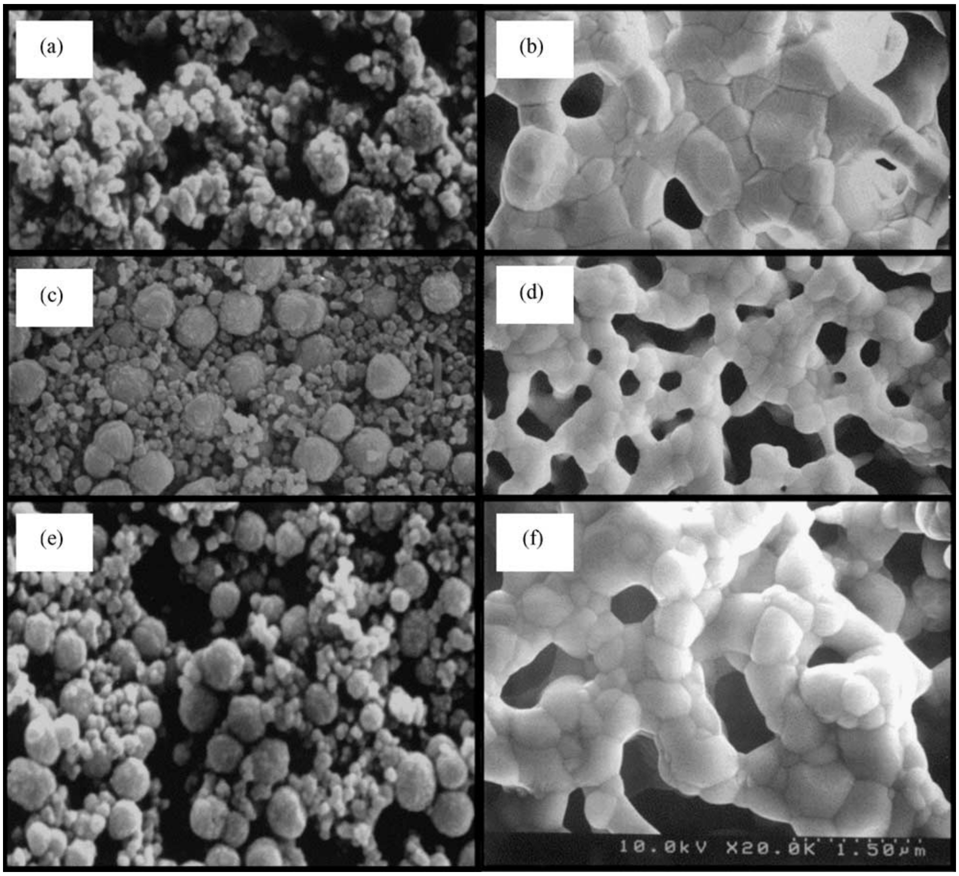

Fig. 2. SEM micrographs showing microstructural variation during sintering for three different electrodes: (a)/(b) the Pt electrode; (c)/(d) the ($La_2Sn_2O_7$ + YSZ)/Pt electrode; and (e)/(f) the ($La_2Sn_2O_7$ + Pt + YSZ)/Pt. Sintering was performed at 1400 °C for 4 h.

on the active site on the electrode, poisoning the electrocatalytic activity for NO. NO conversion begins after pumping out the oxygen adsorbed around the *tpb* as reported by Hibino et al.[3] The bilayered composite electrodes were more effective in NO decomposition than the single-layered Pt electrode as higher current was supplied. This is because that the *tpb* associated with the metal electrode is restricted only to the two dimensional interface between the electrode and the electrolyte compare to composite electrode which has three dimensionally connected *tpb* over whole electrode. Therefore, the Pt|YSZ|Pt cell has a limited number of the F-centers that can form by a partial reduction of YSZ substrate with increasing the applied current density against composite electrode.

For the (LSO + YSZ)/Pt|YSZ|Pt cell, it is believed that the underlying Pt diffuses to some extent into the upper composite layer during sintering. The three dimensionally interconnected porous network structures composed of LSO and YSZ ensures the formation of the oxygen ionic conduction pathway as seen in Fig. 2(d). The diffusion of Pt into such a layer can provide electronic conducting phase. This means that the (LSO + YSZ)/Pt electrode becomes locally a mixed conductor, so that the active site for NO decomposition expands into the upper composite electrode above the underlying Pt layer.

The result of EPMA analysis for compositional variation of the platinum across the (LSO + YSZ)/Pt composite electrode-YSZ electrolyte interface together with SEM micrograph showing the scanned region is presented in Fig. 4. Analysis confirmed that the platinum located between the upper composite electrode and the electrolyte diffused into both interfaces during sintering. The diffusion length of the Pt was much longer ~5 μm into the porous composite layer than into the dense YSZ electrolyte. It is considered that there exists a mixed conducting region ~3 μm down from the top surface in the bilayered (LSO + YSZ)/Pt composite electrode. This makes the electrode more electrochemical active due to the increased effective lengths of the *tpb*.

Intentionally added Pt powders also make the electrode become a mixed conductor expanding three dimensionally the *tpb* into the entire surfaces, which leads to the enhancement in the electrochemical NO decomposition. As shown in Fig. 3, NO conversion was as high as 41% for the (LSO + YSZ + Pt)/Pt|YSZ|Pt cell while the decomposition over the composite electrode without Pt was 20% at 100 mA/cm^2. Higher NO conversion was observed over all the range of applied current density as compared to the (LSO + YSZ)/Pt|YSZ|Pt cell. At lower current density below 60 mA/cm^2, however, the Pt electrode is more electrocatalytically active than (LSO + YSZ + Pt)/Pt. This possibly indicates that the Pt plays another role besides the *tpb* expansion by providing an electronic conduction pathway.

Impedance spectroscopy is utilized to confirm the role of the Pt addition into the electrochemical cell. Fig. 5 shows the impedance spectra of the three types of cells measured in the presence of 0.1% of NO and 2% O_2 at 700 °C. The intercept of the impedance semicircle with the real axis at high fre-

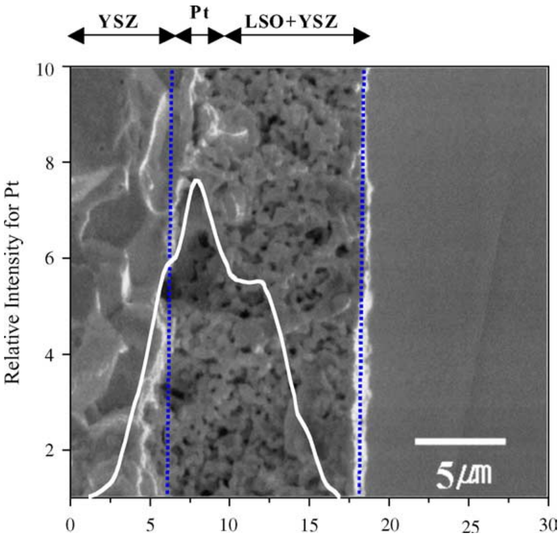

Fig. 4. Compositional variation of platinum across the (LSO + YSZ)/Pt composite electrode-YSZ electrolyte interface with cross sectional SEM micrograph.

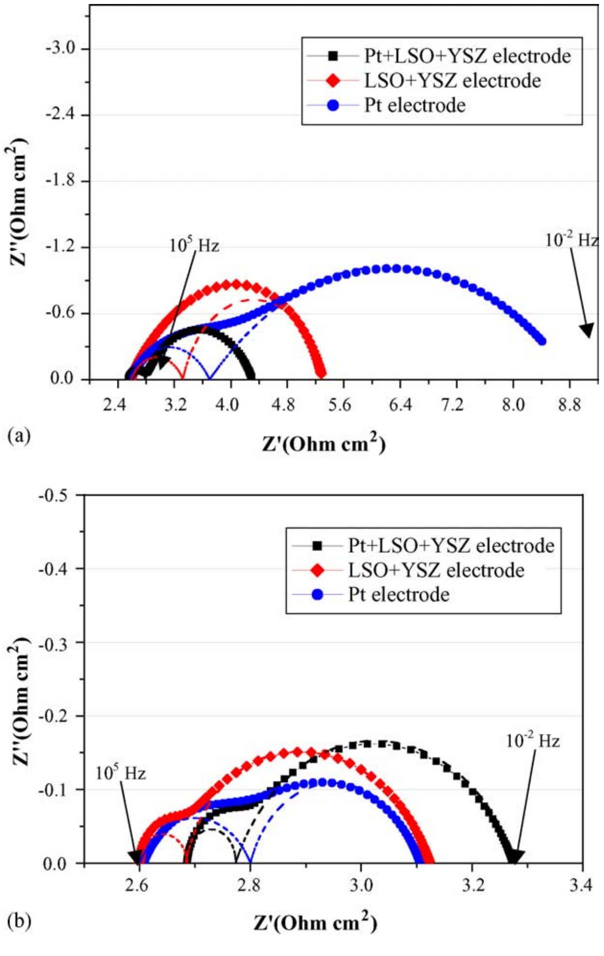

Fig. 5. Impedance spectroscopy for the (LSO + Pt + YSZ)/Pt, ($La_2Sn_2O_7$ + YSZ)/Pt, and Pt electrodes when applied current density is (a) 100 mA/cm^2 (b) 200 mA/cm^2. Measurement was taken at 700 °C.

Table 1
Results of impedance spectroscopy for three electrodes as a function of the current density measured in a reaction atmosphere at 700 °C

Electrode type	Current density					
	Current density = 100 mA/cm^2			Current density = 200 mA/cm^2		
	LSO + YSZ + Pt	LSO + YSZ	Pt	LSO + YSZ + Pt	LSO + YSZ	Pt
Ohmic resistance (Ω cm^2)	2.57	2.58	2.60	2.67	2.68	2.57
Charge transfer resistance (Ω cm^2)	0.24	0.73	1.14	0.08	0.10	0.22
NO conversion (%)	41	22	20	86	85	27

quencies corresponds to the ohmic resistance of the electrochemical cell, which includes the resistance of the electrolyte and the lead wire, whereas the one at low frequencies relates to the total resistance of the cell.[17] In general, the polarization resistance can be given by subtracting the ohmic resistance from the total resistance. In addition, there are observed two semicircles in the impedance spectra, which means that polarization resistance results from two different mechanisms. It is believed that the high frequency arc indicates the charge transfer resistance relating to the electrochemical reduction of either O_2 or NO gases, while the low frequency arc reveals interfacial contact resistance between the electrode and the electrolyte.[18]

Resolved resistances and corresponding NO conversion percentage under different applied current densities are summarized in Table 1. The ohmic resistances for all three electrochemical cells were approximately equal at ~2.6 Ω cm^2 since the same YSZ electrolyte was used. At 100 mA/cm^2, the charge transfer resistance for the ($La_2Sn_2O_7$ + Pt + YSZ)/Pt electrode that decomposes the greater amount of NO was much smaller than for the other two electrodes. The Pt electrode exhibited the largest resistance, nevertheless the NO decomposition ratio was ~22%, similar to that of the ($La_2Sn_2O_7$ + YSZ)/Pt electrode of lower charge transfer resistance. When higher current was supplied to the cell, the charge transfer resistances for both the bilayered composite electrodes further decreased to ~0.1 Ω cm^2 reflecting higher NO decomposition ~85%. However, the Pt electrode still had large resistance and low NO conversion ratio.

The charge transfer resistance is directly correlated to the NO conversion ratio. It relates to the electrochemical reduction rate of either O_2 or NO, which is a strong function of the availability of the F-centers. The numbers of F-centers that can be generated by electrochemical reduction of the oxygen vacancy depend on the applied current and the electrode composition. Under the same lower current applied ~100 mA/cm^2, larger numbers of the electrochemical active sites are expected to form on the mixed conducting ($La_2Sn_2O_7$ + YSZ + Pt)/Pt electrode in which the electronic and ionic conducting phases are spatially well distributed. This results in lower charge transfer resistance and in turn higher NO conversion. High charge transfer resistance associated with the ($La_2Sn_2O_7$ + YSZ)/Pt can be attributed to less reactive sites produced due to the lack of electronic conductivity. Even higher resistance was observed for the Pt electrode since fewer F-centers can form only at the YSZ electrolyte surface. In such a case, the adsorbed oxygen dissociated from either O_2 or NO must diffuse longer to reach active sites, which makes the charge transfer resistance increase. However, the NO conversion ratio over the Pt electrode is similar to that of the ($La_2Sn_2O_7$ + YSZ)/Pt regardless of their being fewer F-centers. This indicates that Pt acts as a catalyst for competitive NO adsorption in the presence of O_2, which enhances the NO conversion ratio even if fewer active sites exist on the electrode surface.

When a sufficient current above 200 mA/cm^2 is supplied, it is believed that the numbers of F-centers become saturated in the case of the ($La_2Sn_2O_7$ + YSZ)/Pt and ($La_2Sn_2O_7$ + YSZ + Pt)/Pt electrodes. This makes both the composite electrodes exhibit low charge transfer resistance and high NO decomposition. However, the Pt electrode still has few reactive sites and its adsorption affinity toward NO does not change with increasing the current, resulting in poor electrochemical activity.

Fig. 6 represents the current efficiency for the electrochemical decomposition of NO over the three electrochemical cells at 700 °C. Current efficiency can be defined as the ratio of the current consumed to decompose NO to N_2 to the total current flux through the electrochemical cell. The current efficiency was zero below 60 mA/cm^2 since only the oxygen was pumped from the cathode to the anode. Above this threshold current density, it sharply increased with the current density and reached a maximum, followed by a decrease. The Pt electrode reached a maximum current efficiency ~1.1% at 60 mA/cm^2, which was higher than for the other composite electrodes at this current density. It was observed that the maximum current efficiency for the bilayered

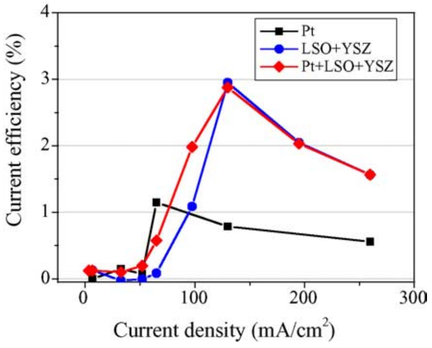

Fig. 6. Current efficiency of NO decomposition as a function of the applied current for difference electrode types at 700 °C.

composite electrodes increased to approximately 3% when a higher current was applied.

4. Conclusions

NO decomposition over an electrochemical cell was investigated with emphasis on its electrode phase composition. The phases and their spatial distribution at the cathode significantly influenced NO decomposition ratio. The electrochemical cell involving the bilayered [($La_2Sn_2O_7$ + YSZ)/Pt] composite electrode could convert more than 85% of NO into N_2 at 200 mA/cm^2 whereas only 27% was decomposed over the platinum electrode. When a lower current ∼70 mA/cm^2 was applied, however, the Pt electrode was more electrochemically active. The addition of Pt into the ($La_2Sn_2O_7$ + YSZ)/Pt] composite electrode not only expands the densities of the *tpb* and the F-centers but also enhances competitive NO adsorption as indirectly confirmed by impedance spectroscopy, both of which promote NO conversion at the lower current density. It is proposed that an electrochemically active cell for NO at less power consumption should involve higher site and number densities for the *tpb* and the F-centers as well as provide a catalyst for selective NO adsorption. Such an electrode should be a mixed conductor with long effective *tpb* lengths and at the same time contain a phase that is easily electrochemically reduced to provide additional oxygen vacancies for the F-centers.

Acknowledgement

This research was supported by a grant (code # 04K1501-01711) from ‘Center for Nanostructured Materials Technology’ under ‘21st Century Frontier R&D Programs’ of the Ministry of Science and Technology, Korea.

References

1. Gur, T. M. and Huggins, R. A., Decomposition of nitric oxide on zirconia in a solid-state elctrochemical cell. *J. Electrochem. Soc.*, 1979, **126**, 1067–1074.
2. Pancharatnam, S., Huggins, R. A. and Mason, D. M., Catalytic decomposition of nitric oxide on zirconia by elctrolytic removal of oxygen. *J. Electrochem. Soc.*, 1975, **122**, 869–875.
3. Hibino, T., Inoue, T. and Sano, M., Electrochemical reduction of NO by alternating current electrolysis using yttria-stabilized zirconia as the solid electrolyte. *Solid State Ionics*, 2001, **130**, 19–29.
4. Hwang, H. J., Moon, J., Matsuda, K., Awano, M. and Maeda, K., Design of multi-layered electrochemical cell for exhaust gas purification. *J. Ceram. Soc. Jpn.*, 2002, **110**, 465–471.
5. Nakamura, T., Sakamoto, Y., Saji, K. and Sakata, J., NO_x decomposition mechanism on the electrodes of a zirconia-based amperometric NO_x sensor. *Sens. Actuators B*, 2003, **7063**, 1–7.
6. Wang, S., Awano, M. and Maeda, K., Synthesis and characterization of dense NiO-(CGO) cathode interlayer for electrocatalytic reduction of NO. *J. Electrochem. Soc.*, 2003, **150**, D209–D214.
7. Zhanga, W.-F., Schmidt-Zhanga, P. and Guth, U., Electrochemical studies on cells M/YSZ/Pt (M = Pt, Pt–Ga_2O_3) in NO, O_2, N_2 gas mixtures. *Solid State Ionics*, 2004, **169**, 121–128.
8. Bredikhim, S., Maeda, K. and Awano, M., NO decomposition by an electrochemical cell with mixed oxide working electrode. *Solid State Ionics*, 2001, **144**, 1–9.
9. Bredikhim, S., Matsuda, K., Maeda, K. and Awano, M., Novel low voltage electrochemical cell for NO decomposition. *Solid State Ionics*, 2002, **149**, 327–333.
10. Matsuda, K., Bredikhim, S., Maeda, K. and Awano, M., Optimization of a composite working electrode for a new family of electrochemical cell for NO decomposition. *J. Am. Ceram. Soc.*, 2003, **86**, 1155–1158.
11. Hwang, H. J. and Awano, M., Preparation of $LaCoO_3$ catalytic thin film by the sol–gel process and its NO decomposition characteristics. *J. Eur. Ceram. Soc.*, 2001, **21**, 2103–2107.
12. Wachsman, E. D., Jayaweera, P., Krishnan, G. and Sanjurjo, A., Electrocatalytic reduction of NO_x on $La_{1-x}A_xB_{1-y}B'_yO_{3-\delta}$: evidence of electrically enhanced activity. *Solid State Ionics*, 2000, **136–137**, 775–782.
13. Teraoka, Y., Torigoshi, K., Yamaguchi, H., Ikeda, T. and Kagawa, S., Direct decomposition of nitric oxide over stannate pyrochlore oxides: relationship between solid-state chemistry and catalytic activity. *J. Mol. Catal. A*, 2000, **155**, 73–80.
14. Subramanian, M. A., High pressure synthesis of pyrochlore-type manganese vanadate and related compositions. *Mater. Res. Bull.*, 1992, **27**, 939–943.
15. Moon, J., Awano, M. and Maeda, K., Hydrothermal synthesis and formation mechanisms of lanthanum tin pyrochlore oxide. *J. Am. Ceram. Soc.*, 2001, **84**, 2531–2536.
16. Park, S., Song, H. S., Choi H.-J. and Moon, J., NO decomposition over the electrochemical cell of lanthanum stannate pyrochlore and YSZ composite electrode. *Solid State Ionics*, 2004, **175**, 625–629.
17. Kim, J.-D., Kim, G.-D., Moon, J.-W., Park, Y., Lee, W.-H., Kobayashi, K., Nagai, M. and Kim, C.-E., Characterization of LSM–YSZ composite electrode by ac impedance spectroscopy. *Solid State Ionics*, 2001, **143**, 379–389.
18. Choi, J. H., Jang, J. H. and Oh, S. M., Microstructure and cathodic performance of $La_{0.9}Sr_{0.1}MnO_3$/yttria-stabilized zirconia composite electrodes. *Electrochim. Acta*, 2001, **46**, 867–874.